# ON THE FLUTTER MECHANISM DRIVEN BY SECOND BENDING-FIRST TORSION COUPLING IN HIGH-ASPECT RATIO WINGS

***Maxime Pirnay*, Edouard Verstraelen, Simon Dosse, Xavier Amandolese and Thomas Andrianne***

**University of Liège,*
*Allée de la découverte 9, Quartier Polytech 1, B52/3, Liège*
*Belgium*

## ABSTRACT

In recent decades, advances in aerospace engineering have intensified research efforts in aeroelasticity. The continuous demand for improved aerodynamic efficiency, reduced fuel consumption, and lower structural mass has led to the development of increasingly flexible wings with high aspect ratios. While these design trends offer significant aerodynamic benefits, they also increase the susceptibility to aeroelastic instabilities, among which flutter remains one of the most critical constraints in wing design [1].

High-aspect-ratio wings are characterized by low-frequency bending modes. When the first two bending modes have natural frequencies lower than that of the first torsional mode, a different type of flutter mechanism involving second bending-first torsion (B2–T1) coupling may occur. This flutter scenario is of particular interest, as it differs from the commonly studied first bending-first torsion coupling and introduces additional complexity related to the node of vibration of the second bending mode, that potentially affects the fluid-structure energy exchanges. The present study combines reduced order aeroelastic modelling and experimental validation to provide physical insight into this instability mechanism.

A reduced-order aeroelastic model is developed by coupling a Rayleigh–Ritz structural formulation with an unsteady aerodynamic model based on Theodorsen's theory [2]. The structural dynamic is represented using a combination of assumed mode shapes derived from the uniform cantilever beam theory, allowing for an efficient and physically meaningful description of bending and torsional deflections. The unsteady aerodynamic forces are considered through frequency-dependent aerodynamic coefficients, enabling the prediction of the modal parameter's variation with airspeed. Based on the predictions of the reduced-order model, experimental wing models were designed and manufactured. The configurations were intentionally tailored to exhibit flutter at flow velocities below the operational limits of the respective wind tunnels. Two wings were built and tested: one in the IAT/Cnam wind tunnel in Paris [3] and the other in the ULiège wind tunnel in Liège [2]. Figure 1 presents photographs of the wings mounted in the wind tunnel, along with the variations of modal frequencies and total damping ratios with airspeed obtained from the reduced-order model and from experimental identification using the covariance-driven SSI method [4].

The experimental results show good agreement with the reduced-order model predictions, both in terms of frequency evolution and damping trends. In particular, the unstable mode exhibits a characteristic "hump" behavior in the damping evolution: as the velocity increases, the damping initially rises before decreasing as the mode progressively transfers energy through modal interactions. At higher velocities, the damping increases again [5]. This non-monotonic behavior differs between the IAT/Cnam and ULiège wings: while the former remains stable over the investigated velocity range, the latter exhibits a clear unstable region.

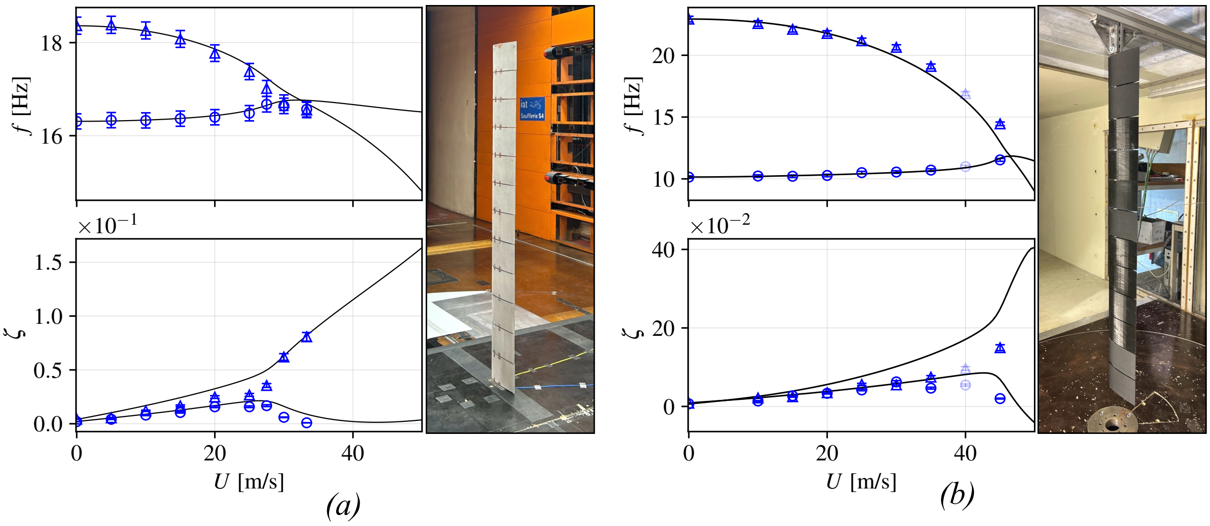

*Figure 1: Experimental and numerical damping and frequency variation with airspeed, together with pictures of the wind-tunnel setup, for (a) IAT/Cnam configuration and (b) ULiège configuration. Experimental data are indicated by blue circles (B2) and blue triangles (T1).*

To further clarify the underlying physical mechanisms, the spatial distribution of aerodynamic energy transfer along the span is analyzed. With increasing reduced velocity, a spanwise change in the sign of the energy exchange is observed, which is attributed to the presence of a vibration node in the second bending mode. This velocity-dependent nodal point modifies the bending–torsion coupling by inducing a redistribution of aerodynamic work along the span, resulting in alternating stabilizing and destabilizing regions as shown in Figure 2. For the ULiège wing, the clearer flutter region is also the consequence of a more pronounced B1 contribution in the unstable aeroelastic mode favorizing a more classical energy exchange and leading to an overall positive fluid–structure energy transfer for $U^* > 5$.

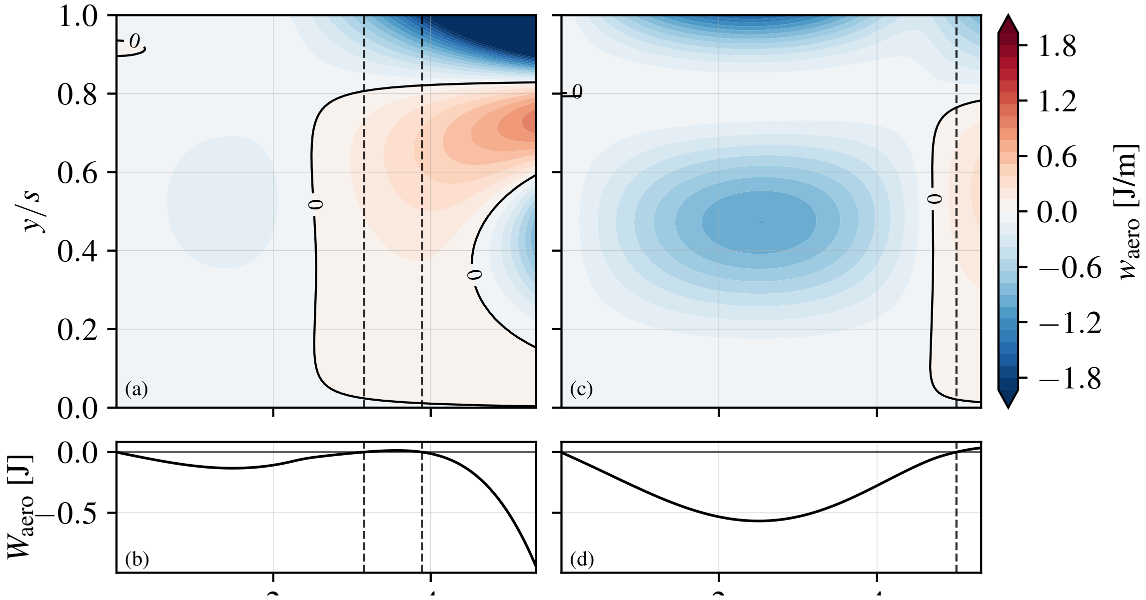

*Figure 2: Space-velocity distributions of aerodynamic work over one vibration period for the flutter mode, together with the corresponding spanwise-integrated aerodynamic work, for IAT/Cnam wing (a-b) and ULiège wing (c-d).*

Overall, this study aims to highlight the importance of higher-order modal interactions in high-aspect-ratio wings and to provide new insight into flutter mechanisms driven by second bending–first torsion coupling. The analysis will be performed using a dimensionless reduced-order model.

# REFERENCES

[1] Afonso, F., Vale, J., Oliveira, É., Lau, F., & Suleman, A. (2017). *A review on non-linear aeroelasticity of high aspect-ratio wings*. Progress in Aerospace Sciences, 89, 40–57. https://doi.org/10.1016/j.paerosci.2016.12.004

[2] Pirnay, M. (2025). *Aeroelastic analysis of a slender wing: Wind tunnel tests and modelling* (Unpublished master's thesis). Université de Liège, Liège, Belgium. Available at: https://matheo.uliege.be/handle/2268.2/23386

[3] Prieur, B. (2023). *Contrôle piézoélectrique des charges et instabilités aéroélastiques sur aile flexible* (Research internship report). École Polytechnique, Paris, France. Conducted at CNAM (LMSSC) under the supervision of X. Amandolèse and B. Lossouarn.

[4] Peeters, B., & De Roeck, G. (1999). *Reference-based stochastic subspace identification for output-only modal analysis*. Mechanical Systems and Signal Processing, 13, 855–878. https://doi.org/10.1006/mssp.1999.1249

[5] Jonsson, E., Riso, C., Lupp, C. A., Cesnik, C. E. S., Martins, J. R. R. A., & Epureanu, B. I. (2019). *Flutter and post-flutter constraints in aircraft design optimization*. Progress in Aerospace Sciences, 109, 100537. https://doi.org/10.1016/j.paerosci.2019.04.001